Influence of Europium Ion on Structural, Mechanical and Luminescence Behavior of Tellurite Nanoglass

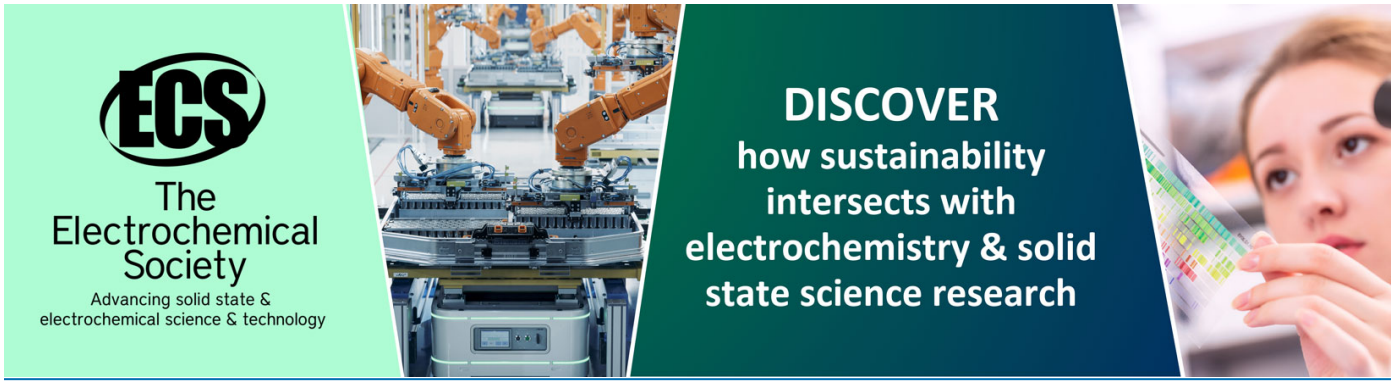

Journal of Physics: Conference Series **431** (2013) 012008 doi:10.1088/1742-6596/431/1/012008

Influence of Europium Ion on Structural, Mechanical and Luminescence Behavior of Tellurite Nanoglass

E S Sazali, M R Sahar and S K Ghoshal
Advanced Optical Material Research Group, Department of Physics, Faculty of Science, Universiti Teknologi Malaysia, 81310, Skudai, Johor Bahru, Johor, Malaysia.

E-mail: mrahim057@gmail.com

Abstract. Understanding the mechanism of enhanced luminescence of rare earth doped glasses in the presence of nanocrystallites and growth kineics is fundamentally important for optical devices. Tellurite nanoglasses of composition (80-x) TeO_2 - 5 Na_2O – 15 MgO – (x) Eu_2O_3, over the concentration region of 0 to 2.5 mol% are prepared using conventional melt-quenching technique. The nanocrystalline particles are obtained by heating the as-cast glass at temperature 15–20°C above the glass crystallization temperature (T_c). The sizes of nanocrystallites are estimated from the X-Ray Diffraction (XRD) pattern using the Scherrer equation having average diameter ~68.7 nm. SEM studies revealed the nanocrystal glass morphology associated with the existence of crystalline phase. The glass density is determined by Precisa Densitometer and the hardness by the Vickers micro-hardness method. The density of tellurite nano-glass is found to be in the range of 5.2413 to 5.4933 g cm^{-3} while the Vickers microhardness varies from 2.77 to 2.93 GPa depending on the dopant concentration. The photoluminescence (PL) spectra exhibits five peaks around 568 nm, 600 nm, 628 nm, 664 nm and 712 nm assigned to $^5D_0 \rightarrow {}^7F_0$, $^5D_0 \rightarrow {}^7F_1$, $^5D_0 \rightarrow {}^7F_2$, $^5D_0 \rightarrow {}^7F_3$ and $^5D_0 \rightarrow {}^7F_4$ transitions respectively. Interestingly, the FWHM and the inverse quality factor of the heat-treated glass are found to decrease with increasing concentration of Eu^{3+} dopants. Our observation may contribute towards the development of solid state lasers.

1. Introduction

The uses of tellurite glasses as a host material have incredibly increased due to their potential applications in laser and fiber [1]. Besides, the understanding of their microscopic mechanism of structural and optical behavior gave much thrust and fundamental interests for both academia and the industries [2]. Interest in tellurite glass containing rare earth element are expected for nonlinear optical devices as for their large third-order nonlinear optical susceptibility [3]. Moreover, the assimilation of rare earth ions can stabilize the metastable crystalline phase which leads to a development of optical devices [4, 5]. Among all glasses, the Eu^{3+} doped tellurite glass has attracted great attention as they can perform persistent spectral hole-burning in the $^7F_0 \rightarrow {}^5D_0$ transition [6]. The integration of rare-earth ions into some kinds of glasses elucidated the significance of rare earth ion-glass host interaction for engineering waveguide devices [7]. Rare earth ions play important role in modern technology as optically active elements in solid state luminescence materials due to the energy levels possessed by these ions when incorporated into a solid state matrix.

The synthesis of nanocrystalline Eu^{3+} doped TeO_2 based glass has not been extensively reported and the growth dynamics of these glass system is far from being understood [8]. Therefore, their

synthesis and understanding the growth behaviors is of considerable technological importance [5]. Moreover, properties of Eu^{3+} doped TeO_2 glasses which undergo heat treatment process are studied only recently. We prepare the tellurite glass doped with europium (Eu^{3+}) via melt quenching technique. The nano-crystalline glass is prepared by the heat-treatment process with nanocrystallites in the host matrix. The effect of dopant concentration on the structural mechanical and optical properties is investigated to study the properties in terms of their compositions.

2. Experimental

The ability of glasses for crystallization is first measured by the values of the glass crystallization temperature (T_c) to obtain transparent glass ceramics. A portion of the glass sample are heat treated for 30 minutes at temperature 15–20°C above T_c in an electrical furnace for all samples. The crystallization of the heat treated samples is identified using XRD (Siemens Diffractometer D5000). The powdered form of the samples is used for diffraction studies. Date are collected in the 2θ range from 15 ° to 75°, in steps of 0.05° and 1s counting time per step using Cu Kα as a radiation source of wavelength λ=1.54056Å. The particle size corresponding to the XRD peak of (111) plane with a cubic structure is estimated from the full width at the half maximum (FWHM), β using Scherrer's equation given by,

$$d = 0.89\,\lambda / \beta \cos\theta \quad (1)$$

where d is the crystallite size, λ is the wavelength and θ is the diffraction angle.

To investigate the kind of the formed crystallites was examined by SEM. The crystallized portion of glass was polished and then successively diamond paste. The specimen is then was coated with a thin layer of carbon by an evaporation technique. An electron accelerating voltage of 8 kV was used and the micrographs were obtained using back-scattered imaging. For the mechanical analysis, the density measurement of glass is made using the Archimedes principle. The density is calculated in gcm^{-3} using,

$$\rho = \frac{W_a}{W_a - W_l}(\rho_l - \rho_a) + \rho_a \quad (2)$$

where ρ is sample density, W_a is weight of sample in air, W_l is weight of sample in liquid, ρ_a is air density (0.001 g cm^{-3}) and ρ_l is liquid density (toluene = 0.8669 g cm^{-3}). By using the value of density, the molar volume, V_m is calculated from,

$$V_m = \left(\frac{M}{\rho}\right) \quad (3)$$

where M is the molecular weight of glass which is calculated from the glass composition. Moreover, the hardness is performed by using the Shimadzu Microhardness Tester HMV-2 with an applied load of the indentor ~9.807N. The Vickers microhardness, H_v is determined from the load applied and the width of the impressed area.

The room temperature luminescence measurement is performed on Nanosecond Luminescence Spectroscopy System, Ekspla Model NT340/1 tunabled Nd: YAG laser system. Each sample in the powder form is placed in the spectrometer and scanned for radiation spectral wavenumber in the range of 200–900 cm^{-1}. The Xenon lamp (300 < λ < 1300nm) was used as a pumping source.

3. Results and Discussion

A series of unheat-treated and heat-treated TeO_2 - Na_2O – MgO glass system doped with Eu^{3+} are successfully prepared by the melt-quenching technique with excellent transparencies.

3.1. X-ray Spectra

Figure 1 shows the XRD pattern for TeO_2 – Na_2O – MgO glass with 1.5 mol% Eu_2O_3 dopant concentrations in which the expected reflections from crystalline particles after heat-treatment are

clearly evidenced. The values of diffraction angle (2θ) of 28.8°, 35.4°, 40.1°, 44.6°, 55.2° and 61.0° confirm the presence of the α-TeO_2 phase (paratellurite) and γ-TeO_2 phase [9]. The particle size in the crystalline phase is estimated from the (FWHM) as shown in the inset of Fig.1 is ~68.7 nm. Indeed the crystallites are nanosized particles. The results indicate that the presence of TeO_2 might play a major role in the phase formation.

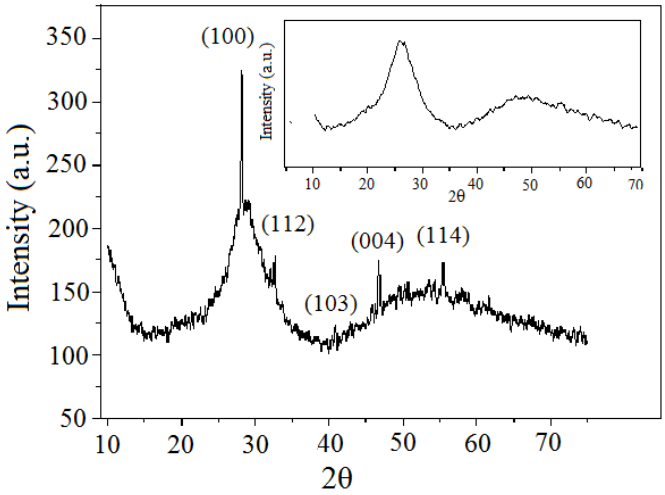

Figure 1. The room temperature XRD spectra for 78.5 TeO_2 – 5 Na_2O – 15 MgO – 1.5 Eu_2O_3 glass after heat-treatment at 442.7°C. The inset shows the XRD patterns for the same nanocrystalline glass in the as-cast condition.

3.2. Structural Properties

The existence of crystalline phase was verified by SEM analysis. Figure 2(a) - (d) shows the SEM micrographs of some TeO_2 – Na_2O – MgO glass systems in varying Eu_2O_3 dopant concentration. Some of them are spherical in shape, some have star-like structure and some of them are irregular in shape. All the micrographs confirm that the crystalline region is composed of TeO_2 phase is dominant.

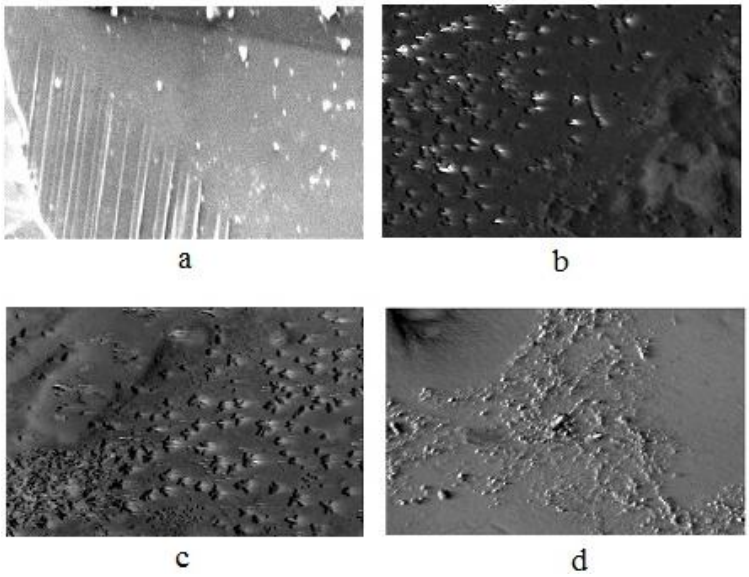

Figure 2. SEM pictures obtained for heat-treated Eu_2O_3 (x) doped glass system above T_c with (a) x = 0, (b) x = 0.5, (c) x = 1.0 and (d) x = 2.0.

Throughout the heat-treated of samples, although the nucleation and growth of nano-crystalline are developed in the same heat-treat operation, but the distribution of nucleates and growth of crystal cannot attain the same extent as the dopant concentration is different. This shows the incorporation of Eu^{3+} dopants with the synthesis of nano-crystalline TeO_2 – Na_2O – MgO glass system. Crystal immersed in the amorphous material, with no observable clustering and a size distribution of are observed.

3.3. Mechanical Properties

Table 1 shows the strong dependence of the glass density on the Eu_2O_3 concentration. The glass density is found to be in the range of 5.2413 g cm^{-3} to 5.4933 g $cm^{-3.}$ As the molecular masses of Eu_2O_3 (351.92) is higher than TeO_2 (159.61), this contributes to higher packing density. The increase in the number of oxygen atoms increases the cation radius. The introduction of Eu^{3+} ions having higher charges and coordination number tend to develop tightly packed glass structure. This result on increasing density is in agreement with others [10]. However, the molar volume in the range of 26.11-25.79 cm^3mol^{-1} shows a decrement as a function of dopant concentration. This might be due to the reduction of total volume size that contributes to the compactness of the glass which is reduced. As the glass undergo the heat-treatment process, the space distance will be decreased leading to a decrease in molar volume.

Meanwhile, it is evident that the Vickers hardness linearly increases from 2.77–2.93 GPa as the concentration of Eu_2O_3 is increased. This may be due to the increasing number of strong covalent bonds from rare-earth dopants causes an increase in the network cross linking in the glasses [11]. The incorporation of Eu^{3+} into the glass system changes the tellurite structure from TeO_4 tbp to TeO_3 bp as more bridging oxygen (BO's) is created that gives more rigidity to the structure and leads as increase in Vickers microhardness [12].

Table 1. Density of Eu^{3+} doped TeO_2 – Na_2O – MgO heat-treated glass system.

Eu_2O_3 (mol %)	Density, ρ (g/cm^3)	Molar Volume, V_m (cm^3/mol)	Hardness, H_v (GPa) ±0.1
0	5.2413 ± 0.016	26.11	2.77
0.5	5.2487 ± 0.019	26.25	2.81
1	5.2827 ± 0.027	26.27	2.86
1.5	5.3011 ± 0.021	26.36	2.88
2	5.4406 ± 0.016	25.89	2.91
2.5	5.4933 ± 0.003	25.79	2.93

3.3. Luminescence Spectra

Figure 3 shows the luminescence spectra of Eu^{3+} doped TeO_2 – MgO – Na_2O for heat-treated glass system as the concentration of Eu_2O_3 increased.

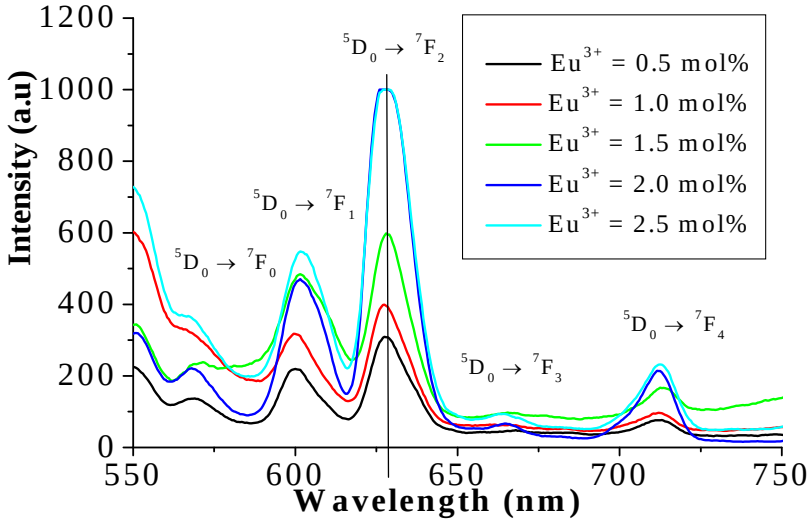

Figure 3. Luminescence spectra of Eu^{3+} doped TeO_2 - Na_2O - MgO heat-treated glass system excited at 400 nm.

Five emission bands corresponding to $^5D_0 \rightarrow {}^7F_0$, $^5D_0 \rightarrow {}^7F_1$, $^5D_0 \rightarrow {}^7F_2$, $^5D_0 \rightarrow {}^7F_3$ and $^5D_0 \rightarrow {}^7F_4$ are evidenced at an excitation wavelength λ_{exci} = 400 nm. Previous report identified the excitation bands at around 355 nm to 395 nm (6, 13, 14). The observed emission peaks of Eu^{3+} doped tellurite glass system at the corresponding transitions cofirmed the presence of europium trivalent state in this glass system which is responsible for the large luminescene efficiency [15].

Figure 4 shows the luminescence spectra of the glass with and without heat treatment at 1 mol% concentration of Eu_2O_3. The detected emission spectra for heat-treated glass sample with the same Eu_2O_3 concentration is similar to the as-cast glass sample which contributes to the same transition. It is clear that the shape of the emission band does not change but there is a slight shift of the peaks position indicating a strong interaction between Eu^{3+} of ions [16].

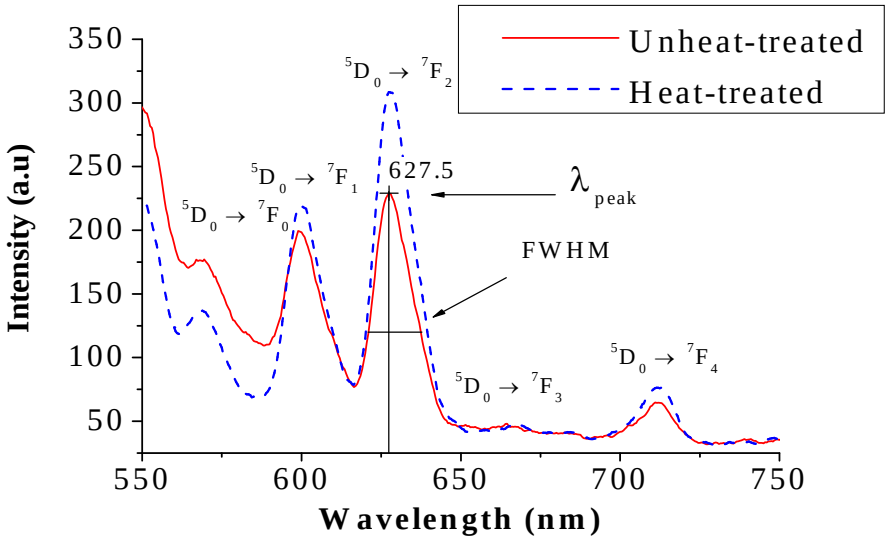

Figure 4. Emission Spectra of glass at 1 mol% of Eu_2O_3 with and without heat-treatment.

The luminescence spectra are further interpreted using the FWHM corresponding to the peak wavelength. This method can be used to indicate the band width ($\Delta\lambda$). Figure 5 shows the average value of FWHM for different transitions for untreated and heat-treated glass samples. The heat-treated glass samples shows more linear changes of FWHM values compared to the un-treated one and is decreased as the Eu_2O_3 dopant concentration is increased except for the $^5D_0 \rightarrow {}^7F_0$ transition. This change is due to the variation of the local structure around lanthanide ion. The increase in the Eu^{3+} ion concentration leads to the changes in the structural unit of the host glass from BO to NBO that contributes to the maximization of Q factor gaving a favorable transition condition for photon to be emitted. Most of the transition that occurs around 600 nm makes the samples best suited for red laser.

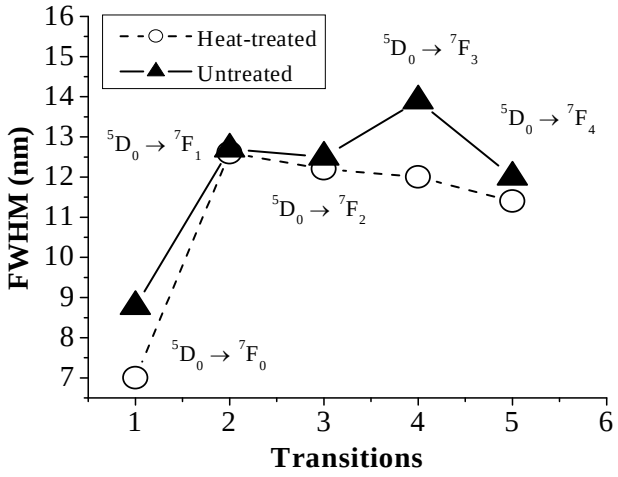

Figure 5. FWHM versus different transitions.

Furthermore, the inverse quality factor Q^{-1} method can be used for emission as described in the Judd Ofelt analysis [17]. A plot of inverse quality factor versus transition for the heat-treated glass samples (Figure 6) shows the decreasing value for the emission transitions $^5D_0 \rightarrow {}^7F_1$, $^5D_0 \rightarrow {}^7F_2$, $^5D_0 \rightarrow {}^7F_3$ and $^5D_0 \rightarrow {}^7F_4$ compared to the un-treated glass system. This result asserts that the Eu^{3+} in the heat-treated tellurite glass system is much promising for laser evelopment. This contributes to higher probability for laser emission of any pumping process.

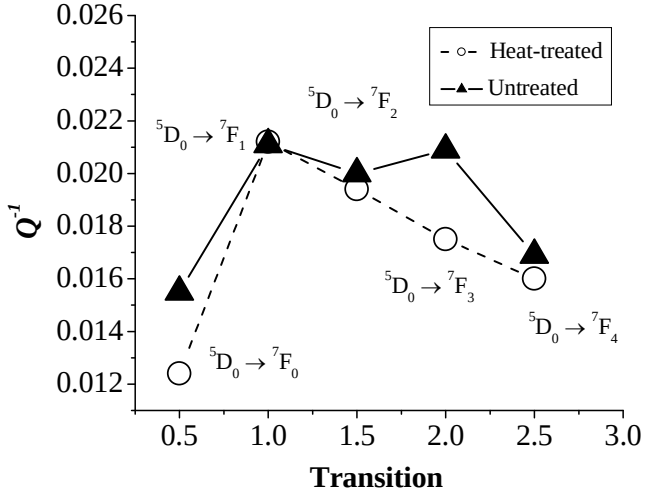

Figure 6. Q^{-1} versus transition for both un-treated and heat-treated samples.

4. Conclusion

A series of nanoglass system based on (80-x) TeO_2 - $5Na_2O$ - 15MgO - (x) Eu_2O_3 for both unheat-treated and heat-treated over the concentration region from 0 to 2.5 mol% are successfully prepared using conventional melt quenching technique. They are mechanically (density and molar volume), structurally and optically (luminescence) characterized. These glasses being largely transparent are of good quality. For the crystallization investigation, XRD spectra confirms the presence of crystalline phase of nano glass which the diameter is estimated around 68.7 nm and SEM studies revealed the nano-crystal glass morphology which is associated to the existence of crystallized phase. Crystal immersed in the amorphous material, with no observable clustering and a size distribution of are observed.The densities are found to be in the range of 5.2413 to 5.4933 g cm^{-3} and increases with increasing the Eu_2O_3 concentration. However, the molar volume varies in the range of 26.11 to 25.79 cm^3mol^{-1}shows a decrement as a function of dopant concentration. In addition, the Vickers hardness is found to increase linearly from 2.77 – 2.93 GPa as the concentration of Eu_2O_3 increased. Luminescence spectra consists of five emission peaks for $^5D_0 \rightarrow {}^7F_0$, $^5D_0 \rightarrow {}^7F_1$, $^5D_0 \rightarrow {}^7F_2$, $^5D_0 \rightarrow {}^7F_3$ and $^5D_0 \rightarrow {}^7F_4$ transitions respectively. The enhancement of Eu^{3+} luminescence especially for the highest emission intensity, $^5D_0 \rightarrow {}^7F_2$ transition lies in the red region as compared to the precursor glass. The heat-treated glass samples shows more linear changes in FWHM and inverse quality factor and is found to decrease with the increase of Eu_2O_3 dopant concentration in comparison to the un-treated glass samples. The role of europium ion of mechanical and spectroscopic properties is understood. Our results may provide valuable information for making nanoglass useful for lasers.

Acknowledgements.
The authors gratefully acknowledge the financial support from Ministry of Higher Education through grant Universiti Teknologi Malaysia under Vot. 06J39, Vot. 06J33 (GUP/MOHE) and MyMaster.

References

[1] Tanabe S *et al* 1990 *J. Non-Cryst. Solids* **122** 79
[2] El-Mallawany R A H *et al* 1995 ESR and electrical conductivity studies of $TeO_2$095CeO2005 semiconducting glasses Materials Chemistry and Physics **41** 87–9
[3] Wang J S *et al* 1994 13μ emission of neodymium and praseodymium in tellurite-based glasses *J. Non-Cryst. Solids* **178** 109-113
[4] Matthew J Dejneka and Alexander Streltsov 2002 Science and Technology Division Corning Incorporated Corning NY 14831
[5] K Hirano *et al* 2001 Rare earth doping into optical nonlinear nanocrystalline phase in transparent TeO2-based glass-ceramics *J. Phys. Chem. of Solids* **62** 2075-2082
[6] Giridhar P *et al* 2011 Spectroscopic studies of RE^{3+} RE =Eu Tb Sm & Dy: lithium lead boro tellurite glasses *ferroelectrics letters* **38** 1–10
[7] Animesh Jha *et al* 2007 Rare-Earth Doped Glass Waveguides for Visible Near-IR and Mid-IR Lasers and Amplifiers *J. Mater. Sci.: Mater Electron* **18** 315–320
[8] Ravi Kumar V *et al* 2001 Structural and Optical Studies of Pr^{3+} Nd^{3+} and Eu^{3+} Ions in Tellurite Based Oxyfluride TeO2-Cif Glasses
[9] Burcu Oz 2006 Thermal Microstructural and Optical Characterization of TeO_2-K_2O Glasses
[10] Yang Li *et al* Hu 2005 *J. Mat. Sci. Tech.* **21** No3 391-394
[11] Kassim A 2010 Physical and Optical Properties of Neodymium and Neodymium Co-Doped Tellurite Glass System PhD Thesis Universiti Teknologi Malaysia
[12] Sahar M R and Sazali E S 2011 Physical and Thermal Properties of TeO_2-Na_2O-MgO Doped Eu_2O_3 Glass UMTAS
[13] Babu P and Jayasankar C K 2000 Optical Spectroscopy of Eu^{3+} Ions in Lithium Borate and Lithium Fluoroborate Glasses *Physica B* **279** 262-281
[14] Luciana R P *et al* 2009 Enhanced luminescence Of Tb^{3+}/Eu^{3+} doped tellurium oxide glass containing silver nanostructures *J. Appl. Phys.* **105** 103505

[15] Ricardo de Almeida *et al* 2008 Eu^{3+} Luminescence in Tellurite Glasses with Gold Nanostructures *Optics Communications* **281** 108–112
[16] Budi Astuti 2005 Study of Optical Properties of $P_2O_5 – Sm_2O_3 – MnO_2$ Glass System Universiti Teknologi Malaysia
[17] Shaik Abdul Saleem *et al* 2011 Erbium-Doped Fluoroborate Glasses for Near Infrared Broadband Amplifiers International *Journal of Applied Glass Science* **2** 215–221